Available online at www.sciencedirect.com
SCIENCE DIRECT
Journal of Power Sources 147 (2005) 196–202
JOURNAL OF POWER SOURCES
www.elsevier.com/locate/jpowsour

A natural-circulation fuel delivery system for direct methanol fuel cells

Q. Ye, T.S. Zhao *

Department of Mechanical Engineering, The Hong Kong University of Science and Technology, Clear Water Bay, Kowloon, Hong Kong, China

Received 5 January 2005; accepted 28 January 2005
Available online 1 April 2005

Abstract

A passive fuel delivery system utilizing a natural-circulation mechanism for direct methanol fuel cells (DMFC) is presented in this paper. It was shown that this novel methanol solution feed system was capable of achieving a performance comparable to that of an actively pumped system for different methanol concentrations ranging from 0.5 to 4.0 M. The theoretical and experimental results showed that the natural-circulation feed flow rate increased with the increase in current density. As a result, the natural-circulation fed DMFC can operate with the fuel delivered in an electrical load-on-demand mode. The feed rates can be optimized for different methanol concentrations by selecting the right tubing size and length of the flow loop. The experimental results also showed that the performance was unstable when the fuel cell operated at low current densities.

Keywords: Direct methanol fuel cell; Anode feeding; Natural circulation; Pumpless

1. Introduction

As one of the most promising candidates for the future power sources of portable applications, direct methanol fuel cells (DMFCs) have attracted considerable attention from both academia and industries, especially over the past 15 years [1–10]. For the state-of-the-art of electrolyte membranes, electrocatalysts, and membrane electrode assemblies (MEAs) utilized in DMFCs, diluted methanol solution is usually used to achieve high power density and energy efficiency. The optimal methanol concentration, however, varies with the operating conditions of a DMFC [6]. Typically, a higher methanol concentration is required at higher current densities, as in this range the anode overpotential is primarily dominated by the mass transport limitation of methanol to the anodic catalyst layer. On the other hand, at low current densities, a lower methanol concentration is preferred because the anode overpotential is dominated by the limitation of the catalytic activity. At low current densities, methanol crossover through the membrane is one of the major factors that cause the cell performance to degrade [9]. Therefore, the requirement of feeding adequate methanol at different current densities makes the design of the fuel delivery system for DMFCs more challenging.

The fuel delivery for DMFCs can be classified into either an active (pumped) or a passive (pumpless) system. For relatively large DMFC systems (several kW, for example), a complete balance-of-plant design [10–12] is preferred to achieve a high power density and energy efficiency, although ancillary pumps and sensors are needed. For small-scale DMFC systems for portable applications, however, a more compact system with no parasitic power consumption is usually desired, and thus a passive fuel delivery system is expected. The simplest design for a complete passive DMFC is to immerse the anode directly into a fuel reservoir and to expose the cathode to the surrounding air (air-breathing) [13–16]. However, there exist two major limitations in this type of

* Corresponding author. Fax: +852 2358 1543.
E-mail address: metzhao@ust.hk (T.S. Zhao).

0378-7753/$ – see front matter © 2005 Elsevier B.V. All rights reserved.
doi:10.1016/j.jpowsour.2005.01.026

passive fuel delivery system. First, since the anode side must be immersed in a fuel reservoir, it is difficult to adopt bipolar flow field plates in the cell stack design. Secondly, the methanol concentration in the catalyst layer is out of control, as the methanol concentration in the reservoir also varies with time.

In this work, taking the advantage of the natural-circulation mechanism, we demonstrated a passive fuel delivery system for the DMFC with a single serpentine flow field, referred to as the natural-circulation fed DMFC hereafter. The performance of this new natural-circulation fed DMFC was tested and compared with that of the conventionally pump fed DMFC.

2. Theoretical analysis of the natural-circulation system

Consider the natural-circulation methanol solution feed system illustrated in Fig. 1, which is essentially similar to traditional natural-circulation systems utilized in boilers [17]. A single DMFC is vertically orientated with its anode inlet on the bottom-left corner and outlet on the top-right corner. A fuel tank is mounted on the top of the cell. Methanol solution is routed from the bottom of the fuel tank to the anode inlet of the DMFC by a tube (inlet tube), while the anode outlet of the DMFC is connected to the fuel tank by another vertical tube (outlet tube), with the distance between the top end of the outlet tube and the bottom of the DMFC denoted by H. Initially, the fuel tank, the inlet and outlet tubes, and the flow field channel are all filled up with methanol solution. As the DMFC discharges, CO_2 gas bubbles are continuously generated, forming a gas–liquid mixture in the anode flow channel and the outlet tube, while the inlet tube is still full of liquid methanol solution. As such, the density difference between the liquid methanol solution in the inlet tube and the two-phase mixture in the remaining section of the flow loop (the anode flow channel and the outlet tube) creates a driven force, which causes a downward flow of methanol solution to the DMFC and an upward flow of the liquid–gas mixture to the fuel tank, where CO_2 gas is separated from methanol solution and vents to ambient via a vent valve at the top of the fuel tank.

In order to identify the major parameters affecting the feed flow rate of the natural-circulation feed system, we present an approximate analysis of the system. A one-dimensional approximation of the force balance among the buoyancy force, the flow resistance, ΔP_F, and capillary force, ΔP_C, through the flow loop yields

$$\rho_l g H - \rho_l (1-\alpha) g H = \Delta P_F + \Delta P_C \quad (1)$$

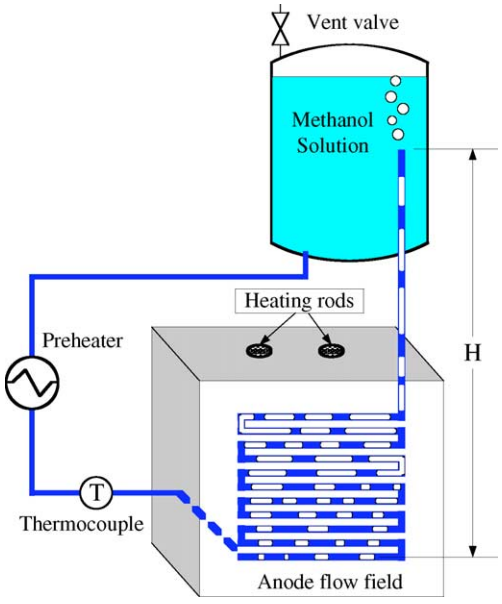

Fig. 1. Schematic representation of the natural-circulation fed DMFC system.

where α is the average void fraction within both the anode flow channel and the outlet tube. Under typical DMFC discharging conditions, we found that slug flow was the predominated flow pattern in both the anode flow channel and outlet tube, as illustrated in Fig. 1. For this reason, the pressure drop in the two-phase region can be assumed to be due to the total flow resistance of gas slugs and liquid slugs. As such, with the assumption of laminar flow, the frictional pressure drop, ΔP_F, can be approximated by

$$\Delta P_F = \frac{32\mu_l}{D_l^2} L_l U_l + \frac{32\mu_l}{D_t^2} L_t (1-\alpha) U_t + \frac{32\mu_g}{D_t^2} L_t \alpha U_t \quad (2)$$

where D and L represent the diameter and length of tubes, with the subscripts l and t denoting the liquid flow section and the two-phase flow section; U_l and U_t represent, respectively, the liquid velocity inside the inlet tube and the two-phase mixture velocity. Note that the first term on the right-hand side of Eq. (2) represents the flow resistance in the liquid flow region, while the last two terms account for the flow resistance in the two-phase flow region. The two-phase mixture velocity U_t can be determined from

$$U_t = \frac{U_l}{1-\alpha} \left(\frac{D_l}{D_t} \right)^2 \quad (3)$$

We now determine the capillary pressure, ΔP_C, due to the contact-angle hysteresis causing gas slugs to resist the liquid flow. As illustrated in Fig. 2, each gas slug is virtually pushed

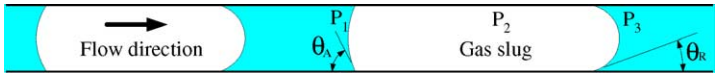

Fig. 2. Contact-angle hysteresis causing gas slugs in a tube to resist the liquid flow.

by the liquid flow to move downstream

$$\Delta P_C = N(P_1 - P_3) = N[(P_2 - P_3) - (P_2 - P_1)]$$
$$= N\left(\frac{4\sigma}{D_t}\cos\theta_R - \frac{4\sigma}{D_t}\cos\theta_A\right)$$
$$= N(\cos\theta_R - \cos\theta_A)\frac{4\sigma}{D_t} \quad (4)$$

where N represents the number of gas slugs and σ is the surface tension of methanol solution. Eq. (4) conceptually describes the capillary force in the tube; as will be shown by the experimental data in this work, this force has a significant effect on the methanol solution feed rate. It should be recognized, however, that a theoretical determination of the capillary force in the entire tube based on Eq. (4) is actually a formidable task because of, at least, two reasons: first, it is difficult to quantify theoretically the number of gas slugs, N. Secondly, the determination of the advancing and receding contact angles in the anode flow field channel consisting of different materials, such as stainless steel, PMMA, and carbon cloth, is also a difficult task. To make the problem tractable, we rewrite Eq. (4) as

$$\Delta P_C = N(\cos\theta_R - \cos\theta_A)\frac{4\sigma}{D_t} = M\frac{4\sigma}{D_t} \quad (5)$$

where M is an empirical constant to be determined by experiments. Substituting Eqs. (2), (3) and (5) into Eq. (1), we obtain

$$\alpha\rho_l g H = \frac{32\mu_l}{D_l^2}U_l\left(L_l + L_t\left(\frac{D_l}{D_t}\right)^4\left(1 + \frac{\mu_g}{\mu_l}\frac{\alpha}{1-\alpha}\right)\right) + M\frac{4\sigma}{D_t} \quad (6)$$

The average void fraction, α, depends on the methanol solution feed rate and the CO_2 generation rate, which is related to the current density, I. Under the condition when the effective height H (300 mm in this work) is much larger than the height of flow field channel (37 mm in this work), the average void fraction, α, can be approximated by

$$\alpha = \frac{1}{U_t A_t}\left(\frac{IA_R}{6F}\frac{RT}{P_{atm} - P_{sat}^{H_2O}}\right) \quad (7)$$

where A_t and A_R represent the outlet tube cross-section area and the active MEA area, respectively. For a given M, solving Eqs. (3), (6) and (7) simultaneously, one can obtain the relationship between the methanol inlet velocity (i.e., the methanol solution feed rate) and discharge current density by eliminating α and U_t. Fig. 3 shows that the variation in the methanol solution feed rate with current density for two different lengths of the inlet tubes (L_l = 0.5 and 2.4 m) with the capillary force neglected (M = 0). Fig. 3 indicates that the methanol solution feed rate increases with the current density. This self-sustained feed flow rate is one of the most remarkable features of this natural-circulation methanol solution feed scheme for a DMFC, as the fuel cell demands higher methanol feed rates with increasing the current density. Moreover, the feed rate can be adjusted by changing the geometric parameters of the system.

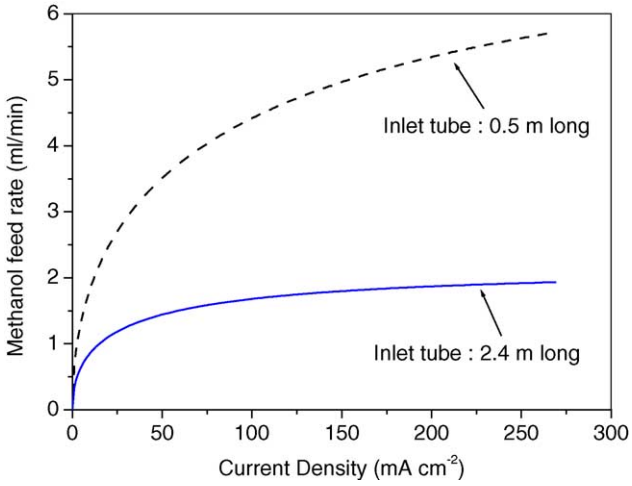

Fig. 3. Calculated methanol feed rates with the capillary force neglected.

3. Experimental

3.1. Membrane electrode assembly (MEA) and cell fixture

A MEA having an active area of 4.0 cm × 4.0 cm was fabricated in-house employing two single-side ELAT® electrodes from E-TEK and a Nafion® 115 membrane. Both anode and cathode electrodes used carbon cloth (E-TEK, Type A) as the backing support layer with 30% PTFE wet-proofing treatment. The catalyst loading on the anode side was 4.0 mg cm^{-2} with unsupported [Pt:Ru]Ox (1:1 a/o), while the catalyst loading on the cathode side was 2.0 mg cm^{-2} using 40% Pt on Vulcan XC-72. The final MEA was formed by hot pressing at 135 °C and 5 MPa for 3 min. The MEA was inserted into an in-house made single cell fixture. To visualize gas evolution and two-phase transport phenomena inside anode flow field channels without sacrificing the convenience and accuracy of temperature control, the cell fixture was made of transparent poly methyl methacrylate (PMMA) for the anode side and aluminum for the cathode side. Both current collector plates were made of stainless steel 316L machined by wire-cut technique. In this study, a single serpentine channel, having 1.3 mm channel width, 1.0 mm rib width and 1.0 mm depth, was formed on both the anode and cathode sides. The final cell assembly is illustrated in Fig. 4.

3.2. Cell test station and test conditions

The cell performance was measured during discharging processes under the staircase voltage controlled mode using an Arbin BT2000 potentiostat–galvanostat electrochemical

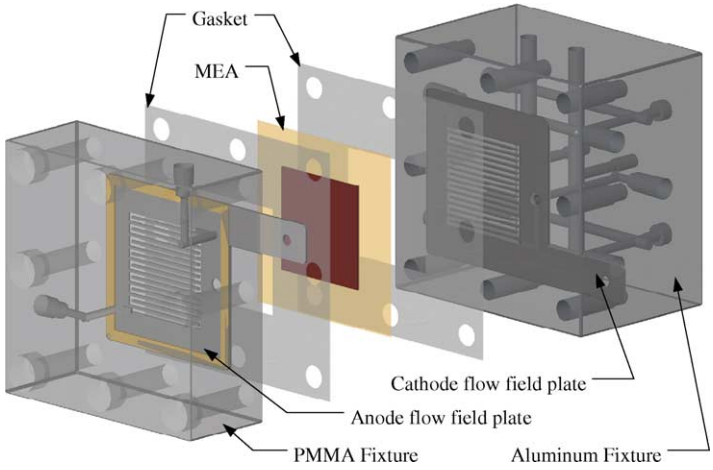

Fig. 4. In-house made DMFC assembly.

testing system. The cell operating temperature as well as the temperature of the methanol solution and oxygen feed were maintained at 60 °C. Unhumidified air was delivered to the cell cathode at ambient pressure and the flow rate was fixed at 250 standard cubic centimeters per minute (sccm) by a mass flow controller (Omega FMA-7105E). In addition to the performance test of the natural-circulation fed DMFC, for comparison the same DMFC was also tested with methanol solution fed by a digital micro-pump (Laballiance, HPLC, Series III). The experiments were carried out by varying methanol concentration from 0.5 to 1.0, 2.0 and 4.0 M and feed flow rates from 0.12 to 8.0 ml min^{-1}.

3.3. Natural-circulation system

As illustrated in Fig. 1, the methanol solution tank had a capacity of 500 ml, which was large enough to maintain a nearly constant methanol concentration for all the experiments in this work. From this tank, 0.25 m FEP tubing (i.d. 1.59 mm) was connected to the flow field outlet and 0.5 m (changed to 2.4 m tubing when 4.0 M methanol was fed to the DMFC) silicone tubing (i.d. 0.89 mm) was connected to the flow field inlet. As illustrated in Fig. 1, a small preheater was installed to preheat methanol solution to a desired temperature (60 °C in this work) before entering the cell. With a distance from the preheater downstream, a thermocouple was inserted into the inlet tube to measure the temperature of methanol solution. It should be recognized that under a given ambient condition the temperature sensed by the thermocouple depends on the methanol solution flow rate only when methanol solution is maintained to an elevated temperature (60 °C in this work) by the preheater. Fig. 5 shows the variation in the measured temperature when methanol solution was pumped by the digital pump at different methanol flow rates. The correlation between the temperature and the flow rate shown in Fig. 5 can be used to determine the feed flow rate furnished by the natural-circulation system when the temperature is measured.

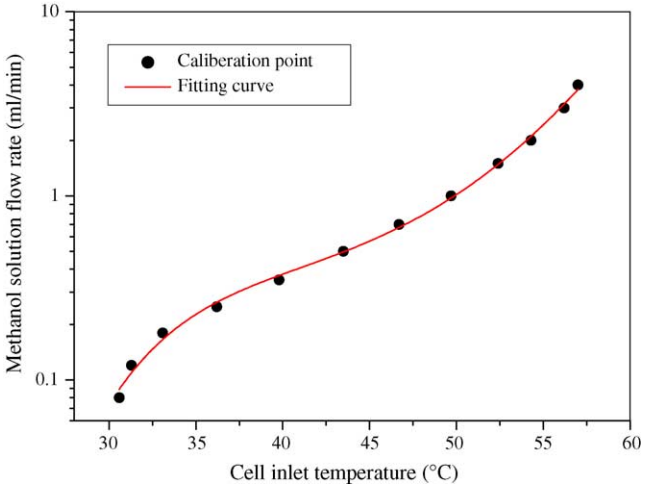

Fig. 5. Calibrated correlation between the methanol solution flow rates and the inlet temperature of methanol solution.

4. Results and discussion

Prior to testing the natural-circulation fed cell, we measured the performance of the pump fed cell with various methanol concentrations at various feed rates. Fig. 6 compares the performance between the natural-circulation fed and the pump fed cells using 0.5 M methanol solution. It is seen that with this lower methanol concentration, the performance of the pump fed cell increased with increasing methanol flow rates, especially at high current densities. It is also noted from Fig. 6 that the performance of the natural-circulation fed cell is closer to that of the pump fed cell at 2.0 ml min^{-1}, indicating that the presently-configured natural-circulation system was unable to supply methanol solution with a sufficient feed rate for the cell with 0.5 M methanol. As shown in Figs. 7 and 8, as the methanol concentration increased to 1.0 and 2.0 M, the pump fed cell exhibited improved performance only at high current densities. The natural-circulation fed cell, however, exhibited

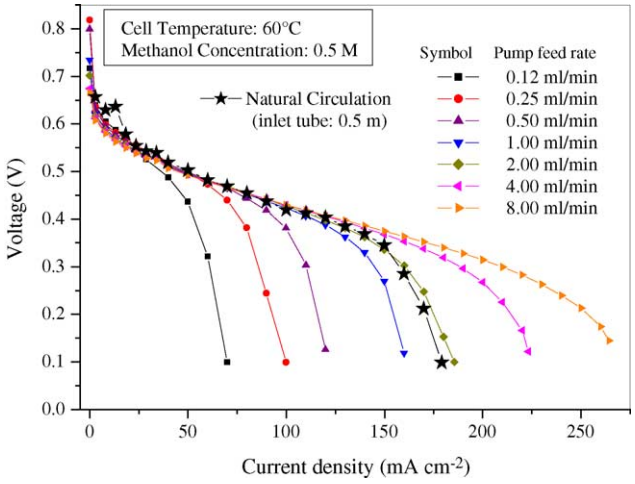

Fig. 6. Comparison between the natural-circulation fed and the pump fed cells with 0.5 M methanol concentration.

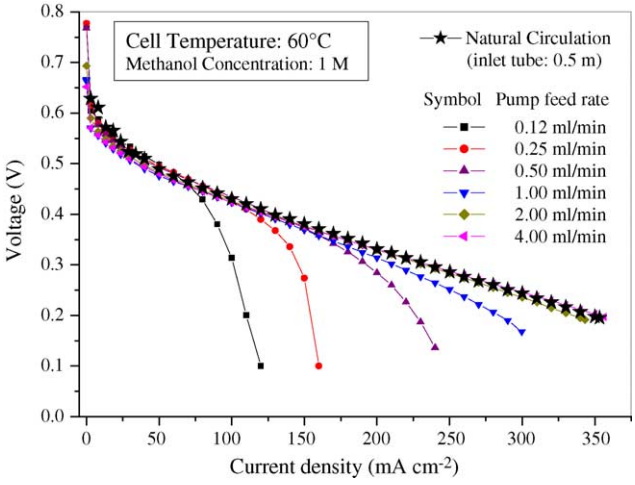

Fig. 7. Comparison between the natural-circulation fed and the pump fed cells with 1.0 M methanol concentration.

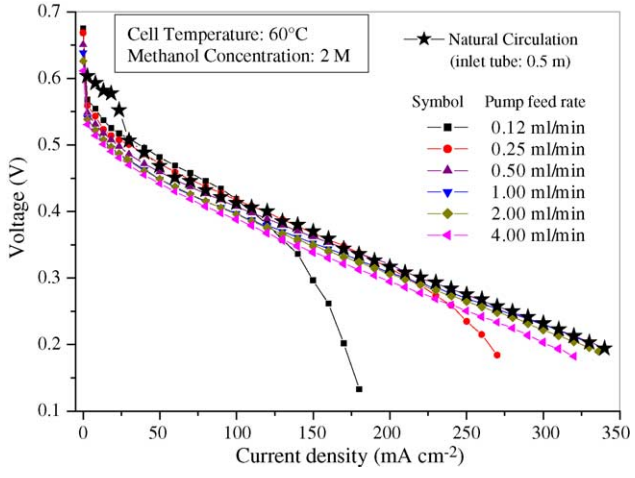

Fig. 8. Comparison between the natural-circulation fed and the pump fed cells with 2.0 M methanol concentration.

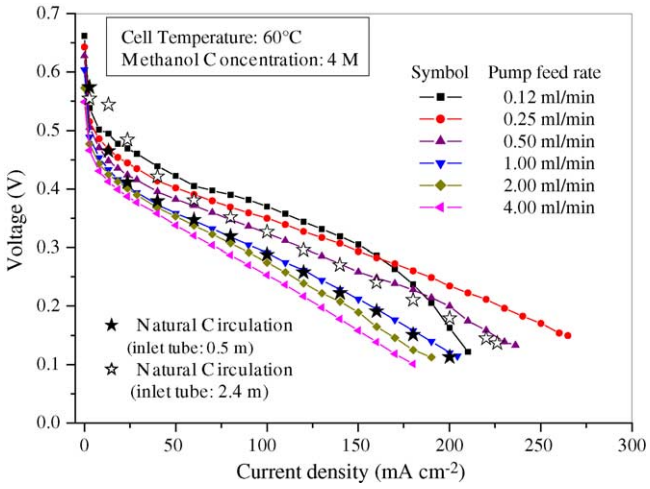

Fig. 9. Comparison between the natural-circulation fed and the pump fed cells with 4.0 M methanol concentration.

better performance than the pump fed cell did at all the tested methanol flow rates within the whole current density range. Fig. 9 shows the performance of both the pump fed and the natural-circulation fed cells with a higher methanol concentration of 4.0 M. As can be seen from this figure, due to the severe methanol crossover, higher methanol solution feed flow rates caused the performance of the pump fed cell to decrease significantly, especially at low current densities. Nevertheless, the cell performance could be maintained relatively higher values when the methanol solution feed rates were kept lower. As seen from Fig. 9, for the pump fed cell, a feed flow rate of 0.12 ml min^{-1} exhibited a better performance, in particular at low current densities. However, the performance of the natural-circulation fed cell fell in the performance range of the pump fed cell with 1.0 and 2.0 ml min^{-1} flow rates at high current densities. This indicates that the flow rate of the natural-circulation feed system with the shorter inlet tube (0.5 m) was too high. To reduce the flow rate of the natural-circulation feed system, the length of inlet tube was increased to 2.4 m. As can be seen from Fig. 9, the performance of the natural-circulation feed system with the longer inlet tube (represented by open star symbols) gave higher performance than that of the system with the shorter inlet tube (represented by solid star symbols) within the entire current density range. During the experiments, it was found that a further increase in the inlet tube length would cause the natural-circulation fed DMFC to halt, especially at low discharge current densities, as the flow resistance would be too large in a longer tube. This is why the performance of the natural-circulation fed cell shown in Fig. 9 could not further be upgraded by reducing the feed rate.

Fig. 10 presents the variation in the natural-circulation feed flow rate with current density corresponding to the cell performance test results shown in Fig. 9. The feed flow rate was determined from the calibration curve presented in Fig. 5 by measuring the inlet temperature of methanol solution. As can be seen from Fig. 10, the longer inlet tube (or larger flow

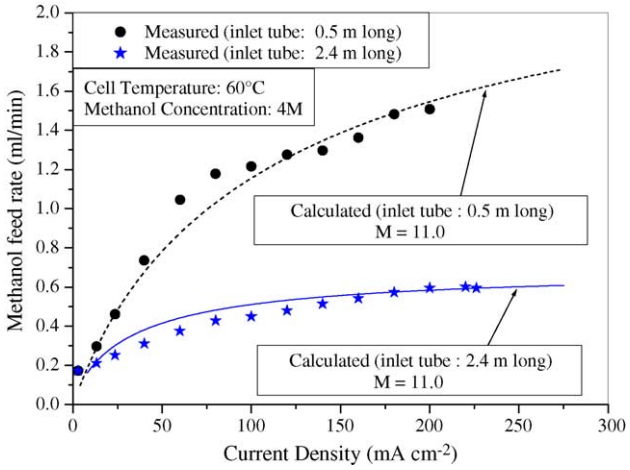

Fig. 10. Variation in the measured methanol solution feed rate with current density.

resistance) exhibited lower methanol solution feed rates. As discussed earlier, for a higher methanol concentration a lower feed rate is required to achieve a better performance. Therefore, the measured feed rates for the longer and shorter inlet tubes presented in Fig. 10 explain why better cell performance was achieved using the longer inlet tube, as shown in Fig. 9.

Fig. 10 also presents the methanol solution feed rate by solving Eqs. (3), (6) and (7) with M set to be 11, which is equivalent to the case with about 30 gas slugs and with the receding and advancing contact angles to be assumed as 30° and 60°, respectively. As can be seen from Fig. 10, the calculated methanol solution feed rates for the two inlet tubes with $M = 11$ fairly fit the measured values. Comparing Figs. 3 and 10 indicates that neglecting the capillary force would lead to a significant error in determining the methanol solution flow rates.

Fig. 11 presents the transient voltage of the natural-circulation fed DMFC measured at different current densities. It can be seen that as the DMFC discharged at the current densities higher than 100 mA cm^{-2}, the cell voltages were relatively stable, meaning that the methanol solution feed rates were stable at high current densities. As the current densities lower than 50 mA cm^{-2}, however, the cell voltages became unstable and the fluctuation amplitude increased with the decrease in current density. These performance fluctuations at low current densities were primarily caused by the fluctuations in the feed rate of the natural-circulation system. As mentioned earlier, the natural-circulation fuel delivery system is virtually driven by the density difference between the pure liquid section and the two-phase flow section. At rather low current densities, the CO_2 bubble generation rate in the DMFC is rather low. Therefore, under such a circumstance the rather small density difference is insufficient to overcome the capillary forces in the flow loop to move methanol solution. However, during this no-flow period, CO_2 bubbles will be accumulated, forming long gas slugs in the two-phase flow section and causing the density difference to increase. Once the density difference becomes sufficiently large, the long gas slugs will be pushed out from the outlet tube and another bubble accumulation period starts. As such, a cyclic bubble accumulation and gas slug removal repeat, causing the feed flow rate to fluctuate.

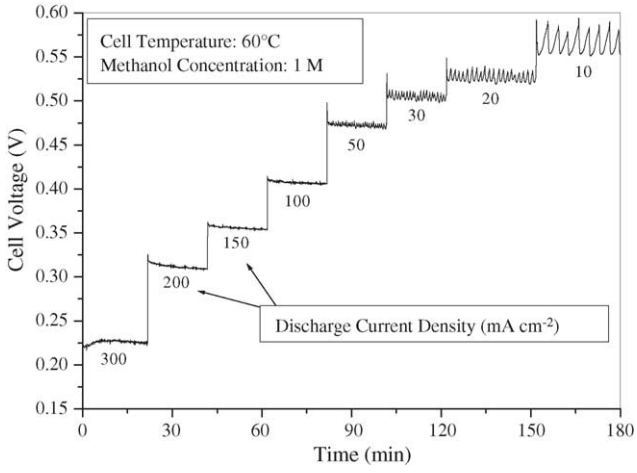

Fig. 11. Voltage fluctuations of the natural-circulation fed cell discharging at various current densities.

During the experiments, we found that the diameter of both the inlet and outlet tubes was an important design parameter. On the one hand, using too small tubes would lead to both a larger flow resistance and capillary force, especially in the two-phase flow region. On the other hand, the inlet tube should be thinner than the outlet tube to prevent gas bubbles from flowing back to the inlet tube, especially at low current densities.

5. Concluding remarks

A natural-circulation fed DMFC was designed, fabricated and tested. It has been shown that this passive fuel delivery system was capable of achieving the performance of the cell with methanol solution fed with a pump, in which the parasitic power is needed. The most striking feature of this new fuel delivery system is that the DMFC can operate with the fuel fed at an electrical load-on-demand mode. This feature is particularly important for the cell performance improvement at low current densities. The natural-circulation fuel delivery system can be optimized for different operating conditions by selecting the right length and size of the inlet and outlet tubes. It also should be mentioned that the performance of the natural-circulation fed DMFC became unstable at low current densities (less than 50 mA cm^{-2}), and there also exists a lower-limit discharge current density (less than 5 mA cm^{-2}), below which the natural circulation is prone to halt due to the limited CO_2 generation rate.

Acknowledgements

The work described in this paper was fully supported by a grant from the Research Grants Council of the Hong

Kong Special Administrative Region, China (Project No. HKUST6197/03E).

References

[1] C.K. Dyer, J. Power Sources 106 (2002) 31.
[2] D. Jollie, Fuel cell market survey: portable applications, Fuel Cell Today 1 (2004).
[3] R. Dillon, S. Srinivasan, A.S. Arico, V. Antonucci, J. Power Sources 127 (2004) 112.
[4] A. Lindermeir, G. Rosenthal, U. Kunz, U. Hoffmann, J. Power Sources 129 (2004) 180.
[5] Q. Ye, T.S. Zhao, H. Yang, J. Prabhuram, Electrochem. Solid State Lett. 8 (2005) A52.
[6] S.C. Thomas, X.M. Ren, S. Gottesfeld, P. Zelenay, Electrochim. Acta 47 (2002) 3741.
[7] M.M. Mench, Z.H. Wang, K. Bhatia, C.Y. Wang, Proceedings of the IMECE 2001, vol. 3, ASME, New York, 2001.
[8] H. Yang, T.S. Zhao, Q. Ye, J. Power Sources 139 (2005) 79.
[9] J. Müller, G. Frank, K. Colbow, D. Wilkinson, Handbook of Fuel Cells—Fundamentals, Technology and Applications, vol. 4, 2003, p. 847.
[10] S. Surampudi, S.R. Narayanan, E. Vamos, H. Frank, G. Halpert, A. Laconti, J. Kosek, G.K. Surya Prakash, G.A. Olah, J. Power Sources 47 (1994) 377.
[11] S.R. Narayanan, T.I. Valdez, Handbook of Fuel Cells—Fundamentals, Technology and Applications, vol. 4, 2003, p. 1133.
[12] S.R. Narayanan, T.I. Valdez, W. Chun, Electrochem. Solid State Lett. 3 (2002) 117.
[13] T. Shimizu, T. Momma, M. Mohamedi, et al., J. Power Sources 137 (2004) 277.
[14] A. Heinzel, C. Hebing, M. Muller, M. Zedda, C. Muller, J. Power Sources 105 (2002) 250.
[15] D. Kim, E.A. Cho, S. Hong, I. Oh, H.Y. Ha, J. Power Sources 130 (2004) 172.
[16] J.G. Liu, G.Q. Sun, F.L. Zhao, G.X. Wang, G. Zhao, L.K. Chen, B.L. Yi, Q. Xin, J. Power Sources 133 (2004) 175.
[17] P. Basu, C. Kefa, L. Jestin, Boiler and Burners, Springer, 2000, pp. 346–371.